Forensic Science International 325 (2021) 110851

Contents lists available at ScienceDirect

Forensic Science International

journal homepage: www.elsevier.com/locate/forsciint

Use of post-mortem chest computed tomography in Covid-19 pneumonia

Fabio De-Giorgio[a,b,*], Francesca Cittadini[a,b], Alessandro Cina[b,c], Elena Cavarretta[d,e], Giuseppe Biondi-Zoccai[d,e], Giuseppe Vetrugno[a,b], Luigi Natale[b,c], Cesare Colosimo[b,c], Vincenzo L. Pascali[a,b]

[a] Department of Health Care Surveillance and Bioethics, Section of Legal Medicine, Università Cattolica del Sacro Cuore, Rome, Italy
[b] Fondazione Policlinico Universitario A. Gemelli IRCCS, Rome, Italy
[c] Department of Diagnostic Imaging, Oncological Radiotherapy and Hematology, Diagnostic Imaging Area, Università Cattolica del Sacro Cuore, Rome, Italy
[d] Department of Medical-Surgical Sciences and Biotechnologies, Sapienza University of Rome, Latina, Italy
[e] Mediterranea Cardiocentro, Napoli, Italy

ARTICLE INFO

Article history:
Received 8 March 2021
Received in revised form 12 May 2021
Accepted 19 May 2021
Available online 27 May 2021

Keywords:
Coronavirus
COVID-19
Pneumonia
Post mortem changes
Post mortem computed tomography
Autopsy

ABSTRACT

Background and aim: COVID-19 is an extremely challenging disease, both from a clinical and forensic point of view, and performing autopsies of COVID-19 deceased requires adequately equipped sectorial rooms and exposes health professionals to the risk of contagion. Among one of the categories that are most affected by SARS-Cov-2 infection are the elderly residents. Despite the need for prompt diagnoses, which are essential to implement all isolation measures necessary to contain the infection spread, deceased subjects in long-term care facilities are still are often diagnosed post-mortem. In this context, our study focuses on the use of post-mortem computed tomography for the diagnosis of COVID-19 infection, in conjunction with post-mortem swabs. The aim of this study was to assess the usefulness of post-mortem whole CT-scanning in identifying COVID-19 pneumonia as a cause of death, by comparing chest CT-findings of confirmed COVID-19 fatalities to control cases.

Materials and methods: The study included 24 deceased subjects: 13 subjects coming from long-term care facility and 11 subjects died at home. Whole body CT scans were performed within 48 h from death in all subjects to evaluate the presence and distribution of pulmonary abnormalities typical of COVID-19-pneumonia, including: ground-glass opacities (GGO), consolidation, and pleural effusion to confirm the post-mortem diagnosis.

Results: Whole-body CT scans was feasible and allowed a complete diagnosis in all subjects. In 9 (69%) of the 13 cases from long-term care facility the cause of death was severe COVID 19 pneumonia, while GGO were present in 100% of the study population.

Conclusion: In the context of rapidly escalating COVID-19 outbreaks, given that laboratory tests for the novel coronavirus is time-consuming and can be falsely negative, the post-mortem CT can be considered as a reliable and safe modality to confirm COVID-19 pneumonia. This is especially true for specific postmortem chest CT-findings that are rather characteristic of COVID-19 fatalities.

1. Introduction

The SARS-CoV-2 outbreak began in the city of Wuhan, Hubei province of China, in December 2019, and rapidly spread around the world. On March 11, 2020, the World Health Organization (WHO) declared a 'pandemic' by WHO Director-General Tedros Adhanom Ghebreyesus [1].

COVID-19 is an extremely challenging disease, both from a clinical and forensic point of view. During the pandemic, the number of autopsies has drastically decreased (by 70%); regardless, the rising number of cases lead to an increase in the number of suspected COVID-19-related deaths at autopsy [4]. Based on the Biological Agents Ordinance, the Committee on Biological Agents has classified SARS-CoV-2 as a risk group 3 pathogen (high individual risk, low community risk) and provided special instructions for managing infected corpses [27]. Nonetheless, biosafety standards in morgues are not on the same level as those applied for infection control in laboratories and clinical environments [5,6].

Abbreviations: GGO, ground-glass opacities; CPP, crazy paving pattern

* Corresponding author at: Department of Health Care Surveillance and Bioethics, Section of Legal Medicine, Università Cattolica del Sacro Cuore, Rome, Italy.
E-mail address: fabio.degiorgio@unicatt.it (F. De-Giorgio).

https://doi.org/10.1016/j.forsciint.2021.110851
0379-0738/

As reported by Cattaneo [10], full autopsies are being performed only in extreme circumstances; targeted dissections are mostly carried out, with percutaneous sampling of fluids. This is due to the low rate of resources and capabilities (around 10%) for the safe management of human remains in European countries [11].

Cattaneo [10] also reported a decreasing trend in terms of criminal proceedings related to traffic and occupational deaths, an increase in the number of lawsuits for medical malpractice, or concerning the liability of medical administrators in relation to the spreading of disease and death. So that in the near future, medico-legal professionals would most likely be asked to examine medical records, collect samples from the dead for evidence of infection and disease, sear for comorbidity and enter the enormous beehive of proving (where possible) if the person contracted COVID-19, whether he or she died of COVID 19 or with COVID-19, and what exactly the causal role of the 30-kilobase virus was [10]. The debate is still open because Finegan O et al. [12] suggested that we should find ways and safe compromises to continue performing medico legal examinations of the dead, while Lacy JM et al. stated that autopsy is unlikely to be necessary in known COVID-19 natural deaths [13]. We fully agree with the above-mentioned authors because if COVID-19 is suspected to be the primary cause of death, first of all we should safeguard the health of mortuary workers [14].

With regard to the diagnosis of COVID-19, the latter is based on the patient's epidemiological history, clinical symptoms, chest imaging findings, and etiological identification of the viral pathogen via nucleic acid detection (swab test) which is considered the gold standard [2]. Real-time reverse transcriptase polymerase chain reaction (rRT-PCR) testing is performed on samples collected from throat swabs, sputum, lower respiratory tract secretions for identification of the viral pathogen via nucleic acid detection [3]. However, this method has some limitations, and a high rate of false negatives can occur [2], so that the role of imaging, in particular chest computed tomography (CT) has become crucial [26].

In the field of forensic medicine, post-mortem computed tomography (PMCT) has been frequently used as a complementary method to autopsy to screen for diseases and trauma, on account of its effectiveness and non-invasiveness [28]. With regard to COVID-19, PMCT can be employed both as a diagnostic and screening tool, to demonstrate the presence of potential disease related pulmonary findings [28]. When used as a screening tool, PMCT may also indicate which way to handle bodies is best. Kniep et al. [30] described patterns of dorsal ground glass opacities (GGO) and consolidations in three fatal cases of COVID-19 using PMCT. COVID-19 pneumonia was confirmed to be the direct cause of death in 2 of the 3 subjects (Case 1 died of sepsis, as a consequence of a superinfected COVID-19 pneumonia). Similarly, Fitzek et al. [27] presented the first German fatality related to SARS-CoV-2-infection. The subject displayed COVID-19-related PMCT findings, as ground-glass density nodules and global multifocal reticular consolidation. In a study by Schweitzer et al. [31], the authors described PMCT findings of a case of fatal SARS-COV-2-positive pneumonia versus those observed in a control case with no acute respiratory distress syndrome. Crazy paving pattern (CPP) with GGO and multifocal consolidations were observed in the infected case. On the contrary, the control case did not display such findings.

In this study, we aim at comparing pulmonary PMCT findings in decedents with and without rRT-PCR confirmed-SARS-CoV2 infection with the purpose of assessing the value of PMCT in diagnosing COVID-19 pneumonia as a potential cause of death.

2. Materials and methods

In the present study, we retrospectively analyzed a consecutive series of 24 decedents with age > 18 year old transferred to our Institute between March 2020 and December 2020.

Twenty-four subjects, both with and without confirmed positive results from SARS-CoV-2 nucleic acid testing of respiratory secretions by oropharyngeal swab, were enrolled in the study. The corpses were divided into two groups: COVID-19 cases or "case group" (N = 13) and "control group" (N = 11). With regard to the subjects belonging to the case group, SARS-CoV2 infection had been confirmed in all cases via rRT-PCR testing; 11 out of 13 COVID-19 cases were diagnosed ante-mortem, and the remaining 2 were diagnosed post-mortem. All case group subjects were transferred to our Institution from long-term healthcare facilities. These subjects presented a clinical history of COVID-19 pneumonia. On the contrary, those of the control group had no ante-mortem history of pneumonia or symptoms of infectious disease and had not been tested for a SARS-CoV2 infection. We acknowledge the possibility that SARS-CoV2 infection without pulmonary involvement might have been present among the subjects of the control group; indeed, although possible, we believe this eventuality was unlikely. Demographic and clinical characteristics of the study population were obtained as for death circumstances.

2.1. Post-mortem computed tomography protocol

Within 48 h after death, whole-body PMCT examination with the corpse in the supine position was performed with Somatom Scope 16-slice CT scann3er, Siemens Healthineers Italia.

The PMCT scans were characterized by the following parameters: 130 kV, 150 mA, 2.5 mm slice thickness, Kernel reconstruction H31S. Implementation of appropriate infection prevention and control measures were arranged in all cases, consisting of appropriate protective garments for technologists carrying out PMCT scan and prompt sanitation of CT facility.

All PMCT images were reconstructed to 1.25-mm thin slices. Multiplanar images were obtained using the multiplanar reformatting (MPR) technique on a workstation (Adwantage Windows 4.7, Generale Electric, USA).

2.2. Image analysis

Every whole-body PMCT examination was read by two radiologists (AC and CC) with 30-years experience in interpreting body CT scan, blinded to results of laboratory test and eventual clinical suspect of COVID-19 infection. In case of discrepancy, they reviewed all CT scans obtained and reached a consensus on findings.

Definitions of radiological terms like ground glass opacity (GGO), crazy-paving pattern, and pulmonary consolidation were based on the standard glossary for thoracic imaging reported by the Fleischner Society [7].

The obtained PMCT scans (Figs. 1–5) showed similarities with chest CT imaging findings of COVID-19 that are typically observed in the living, namely: multiple, bilateral, patchy, sub-segmental, or segmental ground glass opacities (GGO) (Fig. 1) and areas of consolidation, mainly observed along the bronchovascular bundles and subpleural space [8]. Consolidations, on the other hand, are caused by alveolar air being replaced by pathological fluids, cells, or tissues. The latter manifest as pulmonary parenchymal densities that obscure the margins of underlying vessels and airway walls [7], and were found to be indicators of disease progression [9] (Fig. 2). Furthermore, the presence of interlobular septal thickening in the areas of GGO gives rise to the so-called 'crazy paving pattern' [3] (Fig. 3). On chest CT images, COVID-19 shares some similarities with other diseases that can cause viral pneumonia, such as influenza viruses, parainfluenza virus, adenovirus, respiratory syncytial virus, rhinovirus, human metapneumovirus (Fig. 4), and with post-mortem changes [3] (Fig. 5).

2.3. PMCT score

As the presence of GGO or consolidation alone are not predictive of COVID-19 pneumonia at PMCT, since they may be also present as post-mortem changes, we sought to use a semi-quantitative PMCT

Fig. 1. Typical PMCT COVID-19 infection appearance, with bilateral multiple areas of GGO (arrows), without gravitational dependency. Enlarged vessels within GGO areas can also be seen (arrowhead).

scoring that was calculated as follows: 1 point for the presence of one of these findings: GGO, peripheral distribution, bilateral distribution, multilobar distribution, crazy paving pattern, consolidation, absence of gravitational distribution.

2.4. Statistical methods

Continuous variables were expressed as median (1st; 3rd quartile) and categorical variables as N (%) as appropriate. Differences

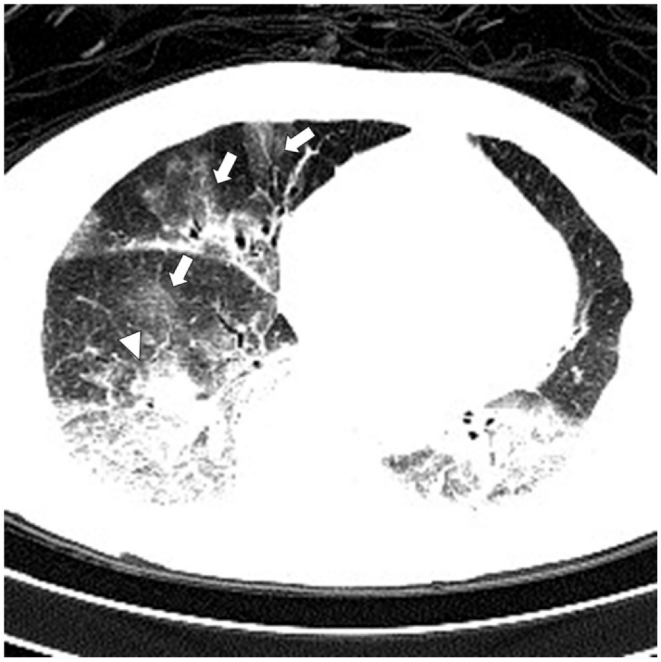

Fig. 2. In a case of PMCT typical GGO of COVID-19 infection in middle and lower right lobe (arrows) were associated to consolidation in lower lobe (arrowhead). The intermediate stage of the disease is characterized by an increase in the number and size of GGOs and a progressive transformation of GGO into multifocal consolidation.

Fig. 3. In PMCT of COVID-19 case we observed in the right lower lobe inter-and intralobular septal thickening (arrohead) superimposed to GGO areas (arrow): the so called "crazy-paving" pattern.

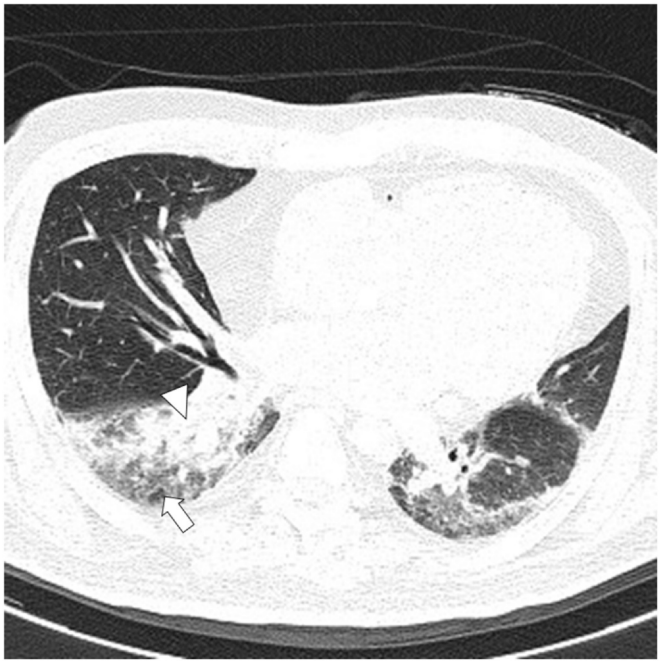

Fig. 4. PMCT in case of pneumonia unrelated to COVID-19 infection. Alveolar consolidation is observed in right lower lobe (arrowhead), surrounded by GGO (arrow). These findings are nonspecific and did not showed the typical distribution of COVID-19 infection.

were assessed using Wilcoxon rank-sum test for continuous variables and Fisher exact test for categorical variables. To determine the optimal cut-off point for PMCT score data were analyzed using receiver operating characteristic curve (ROC), maximizing sensitivity and specificity. Results were expressed as area under the curve (AUC) with 95% confidence intervals (95% CI).

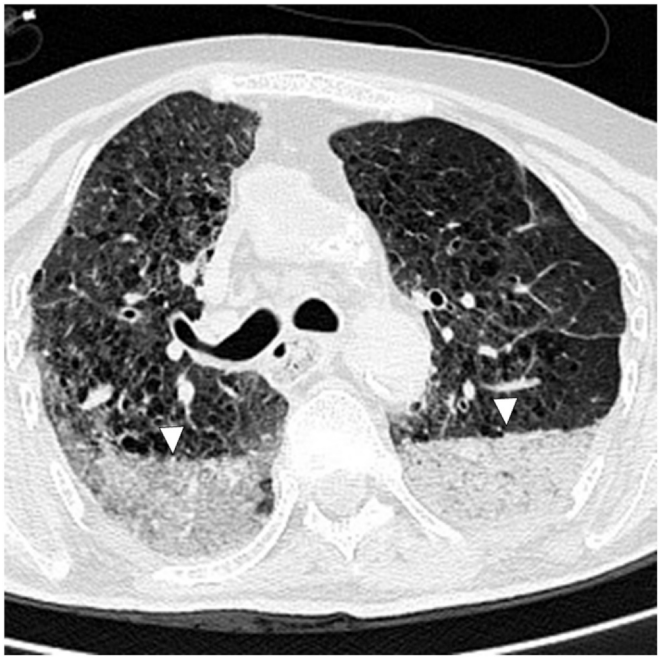

Fig. 5. Increased pulmonary density with a horizontal border, typical for postmortem lung hypostasis, was observed in the dependent region of the bilateral lower lobes (arrowheads); typical GGO signs of COVID-19 infections (not showed) were founded in the same exam in upper lobes.

Statistical significance was set at $p < 0.05$. All analyses were carried out using SPSS, version 17.0 (SPSS, Chicago, IL, USA) and Stata 13 (StataCorp, College Station, TX, USA).

3. Results

3.1. Study population

Twenty-four corpses with an overall age range of 40–101 years (control group, 40–74 years; case group, 86–95 years) were consecutively transferred to our Forensic Institute and included in the study. Thirteen (54%, case group) had died in Healthcare Residences; of the latter, 9 (69.2%) tested positive to SARS-CoV-2 infection on rRT-PCR performed on ante-mortem nasopharyngeal swabs, and 4 (30.8%) tested positive to the infection on rRT-PCR performed on post-mortem nasopharyngeal swabs. The remaining eleven cases (46%, control group) had no history of pneumonia or symptoms of infectious disease and died of causes other than COVID-19 (specifically 3 died of sudden cardiac death, 1 of aortic dissection, 3 of cocaine abuse, 1 of meningioma, 1 of chronic alcohol abuse, 2 of suicide). None of the cases belonging to the control group were tested for SARS-CoV-2 infection, neither ante-mortem nor post-mortem. The study population demographic and clinical characteristics are resumed in Table 1.

3.2. PMCT findings

At PMCT (Table 2), ground-glass opacities (GGO) with bilateral distribution were observed in all (100%) cases, both COVID-19 cases and controls: in 92.3% of cases of COVID-19 cases GGO were peripheral and in 100% were multilobar, versus 27.3% both in No COVID-19 controls ($p = 0.002$ and $p < 0.001$, respectively). In 10/13 (76.9%) of COVID-19 cases gravitational distribution was absent versus 2/11 (18.2%) of controls, $p = 0.012$. A crazy paving pattern (CPP) was depicted in 11/13 COVID-19 cases (84.6%) versus 3/11 (27.3%), $p = 0.011$. Alveolar consolidations did not significantly differ between COVID-19 cases versus controls ($p = 0.408$). An enlargement of vessels within GGO areas, respect to vessels in non-affected parenchyma was present in 10/13 (76.9%) of COVID-19 cases versus 3/11 (27.3%) of controls. Enlarged mediastinal lymphoadenopaties (short axis $>$ 10 mm) and pleural effusion were not statistically different among COVID-19 cases and controls. High pulmonary density on PMCT related to post-mortem changes is characterized by a horizontal, gravity dependent border and is often bilaterally symmetrical (Fig. 5). It should be noticed as in late stage of pulmonary disease characterized by the presence of diffuse interstitial and alveolar involvement (Fig. 6) or massive pleural effusion with atelectasis, the CT evaluation of parenchyma is hindered and a differential diagnosis is almost impossible (see case 12).

3.3. PMCT score

The median PMCT score was 8 (6; 8) for COVID-19 cases and 4 (3; 4) for controls, $p < 0.001$. The area under the Receiver Operating Characteristic (ROC) curve, confidence interval, cut-off point, sensitivity and specificity of the indicators to discriminate COVID-19 versus non-COVID-19 deaths are shown in Table 3. The diagnostic value of parameters was analyzed by the ROC curve. The ROC curve for the PMCT parameters considered in the analysis is shown in Figure ROC (Fig. 7). The most accurate PMCT score cut-off point was 5.5, which yielded a sensitivity of 84.6 and a specificity of 90.9.

Table 1
Demographic and clinical characteristics of the study population.

Feature	No COVID-19 controls (median [1st quartile; 3rd quartile)	COVID-19 cases (median [1st quartile; 3rd quartile)	P value*
Subjects	11	13	–
Age (years)	61 (40; 74)	89 (86; 95)	<0.001
Female gender	1 (9.1%)	11 (84.6%)	0.001
Length	170 (168; 175)	160 (154; 166)	0.012
Weight	70 (62; 83)	60 (55; 68)	0.069
Body mass index	24.2 (22.0; 27.1)	24.1 (20.8; 26.4)	0.580
Ischemic heart disease	5 (45.5%)	9 (69.2%)	0.408
Dementia	0	7 (53.9%)	0.006
Hypertension	1 (9.1%)	6 (46.2%)	0.078
Diabetes mellitus	2 (18.2%)	2 (15.4%)	1
Chronic obstructive pulmonary disease	1 (9.1%)	2 (15.4%)	1
Chronic renal failure	2 (18.2%)	2 (15.4%)	1
Hyatal hernia	0	1 (7.7%)	1
Fever	0	5 (38.5%)	0.041
Pre-mortem nasopharyngeal swab	0	9 (69.2%)	0.001
Post-mortem nasopharyngeal swab	0	4 (30.8%)	0.098

* at Wilcoxon rank-sum test for continuous variables and Fisher exact test for categorical variables.

Table 2
Computed tomography (CT) findings in the study population.

CT	No COVID-19 controls (median [1st quartile; 3rd quartile)	COVID-19 cases (median [1st quartile; 3rd quartile)	P value*61.5
Hours between death and CT scan	8.8 (4.7; 14.2)	47.0 (23.1; 54.0)	0.004
Ground glass opacities	11 (100%)	13 (100%)	1
Peripheral involvment	3 (27.3%)	12 (92.3%)	0.002
Bilateral involvement	11 (100%)	13 (100%)	1
Multilobar involvment	3 (27.3%)	13 (100%)	< 0.001
No gravitational distribution	2 (18.2%)	10 (76.9%)	0.012
Crazy paving pattern	3 (27.3%)	11 (84.6%)	0.011
Consolidations	5 (45.5%)	9 (69.2%)	0.408
Pleural effusion	4 (36.4%)	8 (61.5%)	0.414
PMCT score	4 (3; 5)	7 (6; 8)	< 0.001
Thrombi in pulmonary artery and aorta	3 (27.3%)	1 (7.7%)	0.300
Vessel enlargement	3 (27.3%)	10 (76.9%)	0.038
Lymphoadenopathies	0	2 (15.4%)	0.482
PMCT score	4 (3; 4.5)	7 (6; 8)	< 0.001

* at Wilcoxon rank-sum test for continuous variables and Fisher exact test for categorical variables.

Fig. 6. PMCT in case of COVID-19 infection with diffuse and bilateral interstitial and alveolar involvement. CT findings in similar cases are not specific, as they can be seen in advanced stage of several infectious and non-infectious disease.

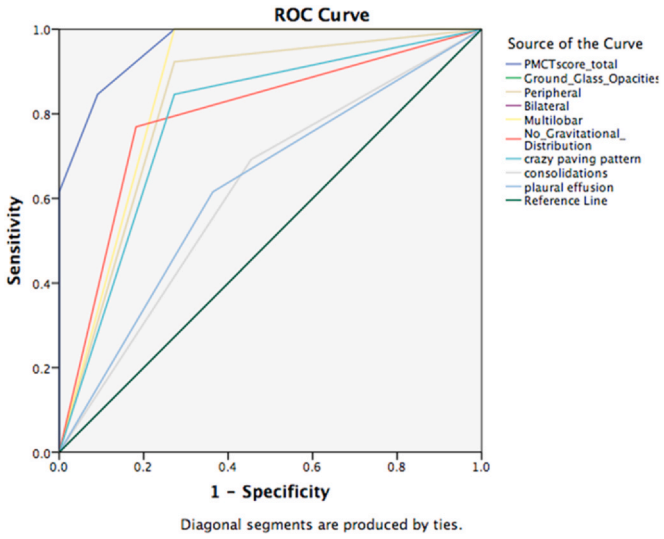

Fig. 7. Receiver Operating Curve (ROC) analysis of the post-mortem computed tomography (PMCT) score in comparison with the single findings. The area under the receiver operating characteristic curve (AUC-ROC) for the PMCT score showed a higher performance than the single PMCT features, demonstrating that PMCT has the potential for post-mortem imaging of lung involvement in COVID-19 infections.

4. Discussion

Knowledge of typical and atypical postmortem lung changes is fundamental in the interpretation of PMCT for the diagnosis of COVID-19, especially since some post-mortem artifacts can mimic pathological conditions and vice versa [17]. The PMCT scans that we obtained (Figs. 1–5) showed similarities with chest CT imaging findings of COVID-19 that are typically observed in the living, such as multiple, bilateral areas of ground glass opacities (GGO) (Fig. 1) and areas of consolidation. Nonetheless, as the presence of GGO or consolidation alone are not predictive of COVID-19 pneumonia at PMCT (since they may be also present as post-mortem changes), we sought to use a semi-quantitative PMCT scoring with the aim of identifying the sensitivity and specificity of given indicators in discriminating between COVID and non-COVID deaths. The latter are

Table 3
Area under the Receiver Operating Characteristic (ROC) curve, confidence interval, cut-off point, sensitivity and specificity of the indicators to discriminate COVID versus non-COVID deaths.

Indicator	Area under the ROC curve (AUC) (95% CI)	cut-off point	Sensitivity	Specificity
PMCT score	0.962 (0.895; 1.0)	5.5	84.6	90.9
Peripheral involvement	0.825 (0.642; 1.0)	0.5	92.3	72.7
Multilobar involvement	0.864 (0.696; 1.0)	0.5	100	72.7
No gravitational distribution	0.794 (0.603; 0.984)	0.5	76.9	81.8
Crazy paving pattern	0.787 (0.591; 0.982)	0.5	84.6	72.7
Consolidations	0.619 (0.388; 0.849)	0.5	69.2	55.5
Pleural effusion	0.626 (−0.397; 0.855)	0.5	61.5	63.

shown in Table 3. Using the PMCT score, we assigned 1 point for the presence of one of these findings: GGO, peripheral distribution, bilateral distribution, multilobar distribution, crazy paving pattern, consolidation, absence of gravitational distribution. The cut-off point of this indicator (PMCT score) was 5.5, which yielded a sensitivity of 84.6 and a specificity of 90.9. The median score was 8 (6; 8) for COVID-19 cases and 4 (3; 4) for controls, $p < 0.001$.

In the absence of chest trauma and lung pathologies, the most common pulmonary finding on PMCT is represented by an attenuation gradient with areas of grater opacity (mainly of ground glass type) in the most dependent regions of the organ (posterior lower lobes) [18,19]. This characteristic finding was observed in 11 subjects (100%) of the control group and 13 (100%) of the case group, with different distribution patterns. In 92.3% of COVID-19 cases GGO were peripheral and in 100% were multilobar, versus 27.3% both in No COVID-19 controls ($p = 0.002$ and $p < 0.001$, respectively). Thus, a statistically significant difference concerning multilobar pulmonary involvement was present between the two groups. The attenuation gradient is related to the presence of typical regional differences in blood and air volume distribution in the lungs. These differences are mainly caused by three post-mortem events: (a) hypostasis, (b) the cessation of tension forces by respiratory muscles, and (b) the pushing action of the diaphragm [20,21]. Some of the GGO can be caused by partial displacement of air, due to the filling of airspaces (pulmonary edema) or as a consequence of interstitial thickening [7]. In the majority of patients, chest CT findings of COVID-19 are mostly compatible with GGO and consolidation; however, the imaging features of the disease vary among different patients and disease stages [22]. In addition, a relatively straight, horizontal demarcation line, separating the area of hypostasis from the anterior non-affected lung, is also commonly observed in the proximity of ground glass opacities (assuming the cadaver is in the supine position) [23,24]. Livor mortis may mimic different types of pathologies, for example: consolidations from infectious or neoplastic processes, aspiration-related findings, edema, atelectasis, pneumonia and contusions [20].

Diffuse bilateral CPP with GGO in areas of reticular densification in a COVID-19 death case were described by Ducloyer et al. [29]. Our results showed CPP in 11/13 COVID-19 cases (84.6%) versus 3/11 (27.3%), $p = 0.011$. This finding represents a rather typical pulmonary change of COVID-19 pneumonia on CT evaluation in the living, which has a tendency towards evolving as the disease progresses [9]. In a study by Helmrich et al. [28], CPP was observed in 9/14 (64%) COVID-19 decedents and identified as a common COVID-19 related finding on PMCT.

Kniep et al. [30] described PMCT findings of three fatal cases of COVID-19; areas of consolidation were observed in 3/3 cases (Case 1 displayed multiple areas of consolidation, Case 2 showed a single area of consolidation and Case 3 displayed peripherally accentuated consolidations). The scans were performed at 48 h, 18 h and 8 h postmortem in Cases 1, 2 and 3, respectively. In another study by Schweitzer et al. [31], the authors compared pulmonary PMCT findings of a case of fatal SARS-COV-2-positive pneumonia, with those of a 24-year old woman control case, with no acute respiratory distress syndrome. The COVID-19-positive subject was a found dead at home over five weeks after first exhibiting possible disease-related symptoms [31]; on PMCT, the subject displayed signs of traction bronchiectasis, multifocal consolidations, CPP with GGO and septal thickening, and small pleural effusions. On the other hand, the control case showed no such signs and only displayed findings of dorsal postmortem hypostasis at the level of the right lung.

In our study population, pleural effusions were observed in 4/11 (36.4%) control group subjects and 8/13 (61.5%) case group subjects, displaying a higher prevalence (although non-significant) in the latter group. Similarly, consolidations were present in 5/11 (45.5%) and 9/13 (69.2%) control and case group subjects, respectively.

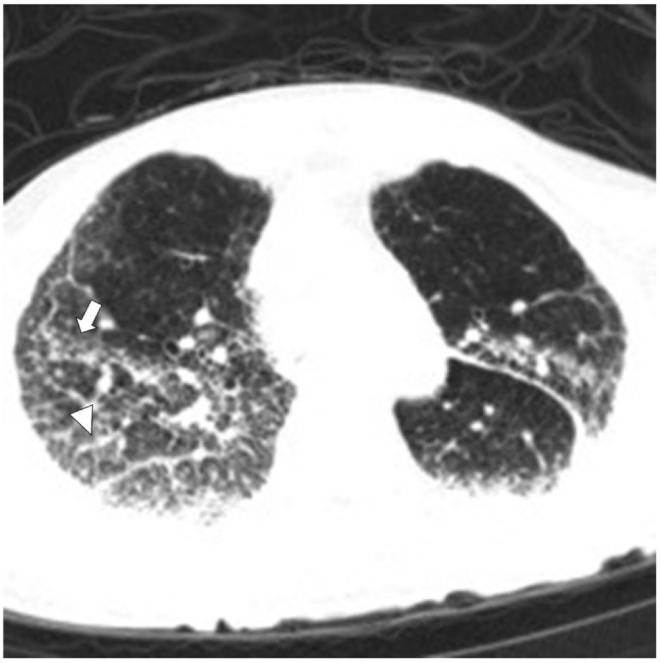

Fig. 8. PMCT, in case with COVID-19 infection and congestive cardiac failure, showed in upper lobes GGO (arrow); bronchovascular bundle and interlobular septa thickening (arrowhead). Pleural effusion and cardiac chambers enlargement were also observed.

Dependent densities are also frequently observed in individuals who die of conditions that result in increased pulmonary venous pressures (i.e., cardiac failure, myocardial infarction, drowning), and who display pulmonary venous congestion and edema [18] (Fig. 8). In the latter patients, however, both extent and severity of densities are greater compared to those commonly observed in the case of normal post-mortem hypostasis. In order to differentiate livor mortis from a pathologic process, a thorough evaluation of the distribution, contours, and presence of associated abnormalities is necessary [20]. Gonoi et al. [25] evaluated 208 lungs of non-traumatic in-hospital deaths using PMCT, with the aim of comparing the findings of non-pathological lungs, with those of lungs with bacterial pneumonia, and lungs with pulmonary edema. In the bacterial pneumonia cases, the following findings were frequently observed: (a) opacities without horizontal plane formation (b) centrilobular opacities, and (c) absence of diffuse bronchovascular bundle thickening. With increasing post mortem interval, the following PMCT findings were observed in healthy, non-pathological lungs: (a) opacities with horizontal plane formation, (b) bilateral symmetric diffuse opacities, (c) diffuse bronchovascular bundle thickening. Thus, in order to identify specific pneumonia or pathology-related changes with PMCT, imaging should be performed as soon as possible after death, in order to reduce the effects of normal postmortem changes. The most commonly observed findings among the pulmonary edema cases were: (a) opacities with horizontal plane formation, (b) diffuse opacities, and (c) interlobular septal thickening [25].

Our results show that the PMCT imaging is a reliable tool for the recognition of COVID-19 related chest changes with high sensitivity and specificity. Therefore, in this historical scenario, we believe that PMCT should still be considered a diagnostic tool to assist post-mortem evaluation, a safe and useful tool to determine the anatomical situation at the time of death, and it should be considered in the event of an exhumation for judicial reasons [16]. In cases where the COVID infection is in a very advanced stage, the general consolidation of the lung does not allow any diagnosis of certainty, but we are persuaded that combining different findings in a PMCT score

would be of great help in identifying with a high specificity those patients who died of COVID infection. In addition, we believe that, in decedents who test positive for SARS-CoV-2, determining the cause of death can be a difficult task for pathologists. This is due to the fact that, while some findings actually represent the true virus-related pathology, others reflect superimposed processes or unrelated illnesses that may act as confounders [15]. In addition, the presence of pulmonary findings on PMCT that are characteristic of COVID-19 pneumonia does not necessarily indicate that COVID-19 is the primary cause of death; in these cases, the role of SARS-CoV-2 as contributing factor or incidental co-morbidity must be thoroughly investigated.

With regard to the limitations of the study we believe that, as this is a hypothesis-generating study, further research is needed to test our score in large consecutive series. Indeed, the number of studied cases was rather low and the PMCT examination of the corpses was limited to 48-hour postmortem; on this account, we believe that it could be useful to extend the examination at, for example, 72-hour postmortem in order to better understand the progression of findings and further assess the diagnostic capability of PMCT in COVID-19 fatality cases. Furthermore, we acknowledge the possibility that SARS-CoV2 infection without pulmonary involvement might have been present among the subjects of our control group, thereby possibly confounding our results. Nonetheless, although possible, we believe this eventuality was unlikely.

5. Conclusion

Our study showed promising results concerning the use of postmortem CT to diagnose COVID infection in conjunction with postmortem swabs. Given that laboratory tests for the novel coronavirus is time-consuming and can be falsely negative, forensic pathologist could play a key role in identifying suspicious post-mortem CT findings based on time interval from the onset of symptoms and guide further evaluation and management of patients. In particular, the use of a semi-quantitative PMCT scoring system (PMCT score) for the identification of both sensitivity and specificity of given indicators in discriminating between COVID-19 and non-COVID-19 deaths proved to be statistically significant. Thus, based on our results, we believe that the identification of specific PMCT findings within 48-hour postmortem may guide coroners and pathologists in the possible diagnosis of COVID-19-related fatalities.

CRediT authorship contribution Statement

Fabio De-Giorgio: Conceptualization, Methodology, Original draft preparation, Writing. **Francesca Cittadini:** Investigation. **Alessandro Cina:** Investigation, Writing, Validation. **Elena Cavarretta:** Investigation, Software, Validation, Writing. **Giuseppe Biondi-Zoccai:** Supervision. **Giuseppe Vetrugno:** Investigation, Supervision. **Luigi Natale:** Investigation, Supervision. **Cesare Colosimo:** Investigation, Supervision. **Vincenzo L. Pascali:** Writing - review & editing.

Declarations of interest

None.

References

[1] World Health Organization, Coronavirus disease (COVID-2019) situation reports. Accessed April 3, 2020.

[2] J. Watson, P.F. Whiting, J.E. Brush, Interpreting a covid-19 test result, BMJ 369 (2020) 1808, https://doi.org/10.1136/bmj.m1808 PMID: 32398230.

[3] W. Yang, A. Sirajuddin, X. Zhang, G. Liu, Z. Teng, S. Zhao, M. Lu, The role of imaging in 2019 novel coronavirus pneumonia (COVID-19), Eur. Radiol. 30 (9) (2020) 4874–4882, https://doi.org/10.1007/s00330-020-06827-4 Epub 2020 Apr 15. PMID: 32296940; PMCID: PMC7156903.

[4] B. Hanley, S.B. Lucas, E. Youd, B. Swift, M. Osborn, Autopsy in suspected COVID-19 cases, J. Clin. Pathol. 73 (5) (2020) 239–242, https://doi.org/10.1136/jclinpath-2020-206522

[5] J.M.E. Pluim, A.J. Loeve, R.R.R. Gerretsen, Minimizing aerosol bone dust during autopsies, Forensic Sci. Med. Pathol. 15 (3) (2019) 404–407, https://doi.org/10.1007/s12024-019-00141-2 PMID: 31342313Free PMC article..

[6] J.M.E. Pluim, L. Jimenez-Bou, R.R.R. Gerretsen, A.J. Loeve, Aerosol production during autopsies: the risk of sawing in bone, Forensic Sci. Int. 289 (2018) 260–267, https://doi.org/10.1016/j.forsciint.2018.05.046 PMID: 29909298Free PMC article.

[7] D.M. Hansell, A.A. Bankier, H. MacMahon, T.C. McLoud, N.L. Müller, J. Remy, Fleischner society: glossary of terms for thoracic imaging, Radiology 246 (2008) 697–722, https://doi.org/10.1148/radiol.2462070712

[8] Z. Ye, Y. Zhang, Y. Wang, Z. Huang, B. Song, C.T. Chest, manifestations of new coronavirus disease 2019 (COVID-19): a pictorial review, Eur. Radiol. 30 (8) (2020) 4381–4389, https://doi.org/10.1007/s00330-020-06801-0 Epub 2020 Mar 19. PMID: 32193638; PMCID: PMC7088323.

[9] F. Pan, T. Ye, P. Sun, S. Gui, B. Liang, L. Li, D. Zheng, J. Wang, R.L. Hesketh, L. Yang, C. Zheng, Time course of lung changes at chest CT during recovery from Coronavirus Disease 2019 (COVID-19), Radiology 295 (3) (2020) 715–721, https://doi.org/10.1148/radiol.2020200370

[10] C. Cattaneo, Forensic medicine in the time of COVID 19: An Editorial from Milano, Italy, Forensic Sci. Int. 312 (2020) 110308, https://doi.org/10.1016/j.forsciint.2020.110308 [Epub ahead of print] PubMed PMID: 32387870; PubMed Central PMCID: PMC7184974.

[11] F.M. Fusco, L. Scappaticci, S. Schilling, G. De Iaco, P. Brouqui, H.C. Maltezou, H.R. Brodt, B. Bannister, G. Ippolito, V. Puro, A 2009 cross-sectional survey of procedures for post-mortem management of highly infectious disease patients in 48 isolation facilities in 16 countries: data from EuroNHID, Infection 44 (1) (2016) 57–64, https://doi.org/10.1007/s15010-015-0831-5 PMID: 26267332.

[12] O. Finegan, S. Fonseca, P. Guyomarc'h, M.D. Morcillo Mendez, J. Rodriguez Gonzalez, M. Tidball-Binz, K.A. Winter, ICRC Advisory Group on the Management of COVID-19 Related Fatalities. International Committee of the Red Cross (ICRC): general guidance for the management of the dead related to COVID-19, Forensic Sci. Int. 2 (2020) 129–137, https://doi.org/10.1016/j.fsisyn.2020.03.007 PMID: 32412013; PMCID: PMC7148714.

[13] J.M. Lacy, E.G. Brooks, J. Akers, D. Armstrong, L. Decker, A. Gonzalez, W. Humphrey, R. Mayer, M. Miller, C. Perez, J.A.R. Arango, L. Sathyavagiswaran, W. Stroh, S. Utley, COVID-19: postmortem diagnostic and biosafety considerations, Am. J. Forensic Med. Pathol. 41 (3) (2020) 143–151, https://doi.org/10.1097/PAF.0000000000000567 PMID: 32379077; PMCID: PMC7202125.

[14] W.R. Webb, N.L. Müller, D.P. Naidich, High-Resolution CT of the Lung, Lippincott Williams & Wilkins, Philadelphia, 2009, pp. 118–128.

[15] L.M. Barton, E.J. Duval, E. Stroberg, S. Ghosh, S. Mukhopadhyay, COVID-19 autopsies, Oklahoma, USA, Am. J. Clin. Pathol. 153 (6) (2020) 725–733, https://doi.org/10.1093/ajcp/aqaa062 MID: 32275742.

[16] F. Cittadini, F. De-Giorgio, A. Cina, V.L. Pascali, Reliable postmortem computed tomography scan diagnosis of COVID-19 pneumonia, Am. J. Forensic Med. Pathol. 41 (3) (2020) 239–240, https://doi.org/10.1097/PAF.0000000000000594 PMID: 32604146.

[17] L. Filograna, M.J. Thali, Post-mortem CT imaging of the lungs: pathological versus non-pathological findings, Radio. Med. 122 (12) (2017) 902–908, https://doi.org/10.1007/s11547-017-0802-2 Epub 2017 Aug 23. Review. PubMed PMID: 28836139.

[18] S. Shiotani, M. Kohno, N. Ohashi, K. Yamazaki, H. Nakayama, K. Watanabe, Y. Oyake, Y. Itai, Non-traumatic postmortem computed tomographic (PMCT) findings of the lung, Forensic Sci. Int. 139 (2004) 39–48.

[19] H. Hyodoh, J. Shimizu, S. Watanabe, S. Okazaki, K. Mizuo, H. Inoue, Time-related course of pleural space fluid collection and pulmonary aeration on postmortem computed tomography (PMCT), Leg. Med. (Tokyo). 17 (4) (2015) 221–225, https://doi.org/10.1016/j.legalmed.2015.01.002 Epub 2015 Jan 21. PubMed PMID: 25657038.

[20] A.D. Levy, H.T. Harcke, C.T. Mallak, Postmortem imaging: MDCT features of postmortem change and decomposition, Am. J. Forensic Med. Pathol. 31 (1) (2010) 12–17, https://doi.org/10.1097/PAF.0b013e3181c65e1a Review. PubMed PMID: 20010292.

[21] S. Shiotani, T. Kobayashi, H. Hayakawa, K. Kikuchi, M. Kohno, Postmortem pulmonary edema: a comparison between immediate and delayed postmortem computed tomography, Leg. Med. (Tokyo) 13 (3) (2011) 151–155, https://doi.org/10.1016/j.legalmed.2010.12.008 PubMed PMID: 21315646.

[22] M. Chung, A. Bernheim, X. Mei, N. Zhang, M. Huang, X. Zeng, J. Cui, W. Xu, Y. Yang, Z.A. Fayad, A. Jacobi, K. Li, S. Li, H.C.T. Shan, Imaging features of 2019 Novel Coronavirus (2019-nCoV), Radiology 295 (1) (2020) 202–207, https://doi.org/10.1148/radiol.2020200230 Epub 2020 Feb 4. PMID: 32017661; PMCID: PMC7194022.

[23] M. Ishida, W. Gonoi, H. Okuma, G. Shirota, Y. Shintani, H. Abe, Y. Takazawa, M. Fukayama, K. Ohtomo, Common postmortem computed tomography findings following atraumatic death: differentiation between normal postmortem changes and pathologic lesions, Korean J. Radiol. 16 (4) (2015) 798–809, https://doi.org/10.3348/kjr.2015.16.4.798 Epub 2015 Jul 1. Review. PubMed PMID: 26175579.

[24] A. Christe, P. Flach, S. Ross, D. Spendlove, S. Bolliger, P. Vock, M.J. Thali, Clinical radiology and postmortem imaging (Virtopsy) are not the same: Specific and unspecific postmortem signs, Leg. Med. (Tokyo). 12 (5) (2010) 215–222, https://doi.org/10.1016/j.legalmed.2010.05.005 Epub 2010 Jul 13. PubMed PMID: 20630787.

[25] W. Gonoi, Y. Watanabe, G. Shirota, H. Abe, H. Okuma, Y. Shintani-Domoto, T. Tajima, M. Fukayama, O. Abe, M. Ishida, Pulmonary postmortem computed tomography of bacterial pneumonia and pulmonary edema in patients following non-traumatic in-hospital death, Leg. Med. (Tokyo). 45 (2020) 101716, https://doi.org/10.1016/j.legalmed.2020.101716 Epub ahead of print. PMID: 32442911.

[26] J.P. Kanne, H. Bai, A. Bernheim, M. Chung, L.B. Haramati, D.F. Kallmes, B.P. Little, G. Rubin, N. Sverzellati, COVID-19 imaging: what we know now and what remains unknown, Radiology 299 (2021) 262, https://doi.org/10.1148/radiol.2021204522 Epub ahead of print. PMID: 33560192; PMCID: PMC7879709.

[27] A. Fitzek, J. Sperhake, C. Edler, A.S. Schröder, A. Heinemann, F. Heinrich, A. Ron, H. Mushumba, M. Lütgehetmann, K. Püschel, Evidence for systematic autopsies in COVID-19 positive deceased: case report of the first German investigated COVID-19 death, Rechtsmedizin (Berl) (2020) 1–6, https://doi.org/10.1007/s00194-020-00401-4 Epub ahead of print. PMID: 32836897; PMCID: PMC7247437.

[28] E. Helmrich, L. Decker, N. Adolphi, Y. Makino, Postmortem CT lung findings in decedents with Covid-19: a review of 14 decedents and potential triage implications, Forensic Imaging 23 (2020) 200419, https://doi.org/10.1016/j.fri.2020.200419 Epub 2020 Nov 5. PMCID: PMC7643627.

[29] M. Ducloyer, B. Gaborit, C. Toquet, L. Castain, A. Bal, P.P. Arrigoni, R. Lecomte, R. Clement, C. Sagan, Complete post-mortem data in a fatal case of COVID-19: clinical, radiological and pathological correlations, Int J. Leg. Med. 134 (6) (2020) 2209–2214, https://doi.org/10.1007/s00414-020-02390-1 Epub 2020 Aug 6. PMID: 32767018; PMCID: PMC7410356.

[30] I. Kniep, A. Heinemann, C. Edler, J.P. Sperhake, K. Püschel, B. Ondruschka, A.S. Schröder, COVID-19 lungs in post-mortem computed tomography, Rechtsmedizin (Berl) (2021) 1–3, https://doi.org/10.1007/s00194-021-00462-z Epub ahead of print. PMID: 33612977; PMCID: PMC7884063.

[31] W. Schweitzer, T. Ruder, R. Baumeister, S. Bolliger, M. Thali, E. Meixner, G. Ampanozi, Implications for forensic death investigations from first Swiss post-mortem CT in a case of non-hospital treatment with COVID-19, Forensic Imaging 21 (2020) 200378, https://doi.org/10.1016/j.fri.2020.200378 Epub 2020 Apr 18. PMCID: PMC7166113.